

Response Calculations of the CdZnTe Detector Using EGS4 ¹

J. C. Liu, W. R. Nelson and R. Seefred

*Stanford Linear Accelerator Center,
MS 48, P. O. Box 4349, Stanford, CA 94309, USA*

Abstract

The spectral response of a CdZnTe semiconductor detector has been calculated with the EGS4 Code System. The latest low-energy photon production and transport routines developed at KEK, which consider the K and L shell fluorescent photon production in compounds, bound Compton scattering, Doppler broadening, etc., were included in the EGS4 code. The calculations of the CdZnTe detector also took into account the collection efficiency of the produced electron-hole pairs (described by Hecht equation) and the modification on spectral peaks due to both the Fano factor and electronic-noise broadening. The calculated results are compared with measurements made with encapsulated ²⁴¹Am and ¹³⁷Cs disk sources. It was found that, by trying various mobility-lifetime values for holes, the calculated spectral response still did not have perfect agreement with measurements.

1 Introduction

In a previous study[1], the EGS4 Code System[2] was used to calculate the spectral response for a CdZnTe detector (called CZT hereafter) that was used to measure the synchrotron radiation leakage spectra in a PEP-II accelerator radiation environment. In that paper, minor disagreements were found when the EGS4-calculated photon spectra were compared with measurements made using encapsulated ²⁴¹Am, ¹³³Ba and ¹⁰⁹Cd disk sources.

In the previous study, the following processes were standard with EGS4: photoelectric effect (with angular sampling from the Sauter formula), coherent (Rayleigh) and Compton scattering (unbound), discrete Moller and Bhabha interactions, positron annihilation (in-flight and at-rest), continuous energy loss, Moliere multiple scattering applied to charged-particle tracks, and pair production/bremsstrahlung (with angular sampling). In addition to these processes, the simulations also specifically took into account:

1. production of K-shell fluorescence from a CZT mixture, using an improvement to a method developed for EGS4 by Del Guerra et al[3],
2. collection of electron-hole pairs (the signal) using the Hecht equation[4],
3. narrowing of the signal by considering Fano factor and broadening of the signal due to electronic-noise.

Recently Hirayama and Namito at KEK have developed routines to treat low-energy photon production and transport in materials[5, 6]. The routines mainly consider bound Compton scattering, Doppler broadening, and the K and L shell fluorescent photon production in elements, as well as in compounds. Therefore, in this study we incorporated the KEK routines into the EGS4 Code System in order to compare with the previous study. In addition, to further resolve the above-mentioned

¹Work supported by the US Department of Energy under contract DE-AC-03-76SF00515

discrepancy between EGS4 calculations and measurements, this time we have studied in depth the calculation algorithm of spectral response, particularly by using various mobility-lifetime values in the Hecht equation. Additional photon spectra measurements using ^{241}Am and ^{137}Cs disk sources were also made to compare with EGS4 calculations.

2 EGS4 Calculations

2.1 Detector Material and Energy Cutoffs

The CZT detector was made by eV Products, Inc. (model eV-180-3-3-2-S; 375 Saxon Blvd., Saxonburg, PA 16056, USA). The CZT material data was created with the MIXT option of PEGS4 using a density of 5.86 g/cm^3 and RHOZ values of 50.58, 3.27 and 63.80 for Cd, Zn and Te, respectively (corresponding to atomic percentages of 45, 5 and 50%). The PEGS4 energy limits were chosen to be (AP=0.001, UP=10.0) and (AE=0.521, UE=10.511) MeV for photons and electrons, respectively. In addition to turning on the Rayleigh scattering option (IRAYL=1) and the option of radiative stopping powers compliant with ICRU-37 (IAPRIM=1), all the KEK low-energy photon options (IXRAY=1, IBOUND=1, INCOH=1, ICPROF=-3, IMPACT=1) were turned on.

The photon transport cutoff PCUT was set at 0.001 MeV. The electron cutoff energy ECUT was set at 1.511 MeV, forcing the kinetic energy of the electrons to be deposited at their points of creation, except for ^{137}Cs (ECUT was then 0.561 MeV). The rationalization for doing this is based on the fact that the ranges of secondary electrons from all radioisotopic source photons (except ^{137}Cs) in CZT are much smaller than the dimensions of the CZT crystal. In any case, a check was made with ECUT=AE=0.521 MeV (i.e., 10 keV kinetic energy) and the results were essentially the same as with higher ECUT values. It was also found that the use of PRESTA[7] did not change the results.

2.2 Measurements and EGS4 Geometry

The measurement and the corresponding EGS4 geometry in this study (see Figure 1) were similar to that in the previous study. X-ray photographs showed that the CZT crystal ($3\times 3\text{ mm}^2$ and 2 mm thick), mounted inside a BNC-type connector, is 0.575 cm from the 0.25-mm-thick beryllium window of CZT detector. An aluminum cylinder of 0.45 cm inner radius and 0.1 cm thickness surrounds the crystal. Our EGS4 user code utilized a generalized cylinder/azimuthal plane/slab geometry package (ucRTZ.mortran and ucRTZ.data), with the cylindrical radius of the CZT crystal chosen to be 0.17 cm to provide an equivalent cross-sectional area of 9 mm^2 . The ^{241}Am or ^{137}Cs disk source was positioned at 10 cm away from the beryllium window. The radiation sources were sealed in plastic discs, 25 mm in diameter and 5 mm thick (the source was actually about 1 mm deep).

The input gamma and X-ray energies, and their corresponding intensities, were taken from ICRP Publication 38[8] for each of the three sources: ^{241}Am , ^{133}Ba and ^{109}Cd . A single energy of 662 keV was used for ^{137}Cs source. Energy sampling was done by means of a simple cumulative distribution table. Due to the large distance, a point source and a monodirectional photon beam toward the front face of CZT detector were assumed in the calculations.

To reduce electronic noises, the BNC-CZT unit was attached directly to a matching connector on an inverting low-noise, charge-sensitive preamplifier (eV Products, model eV-550). A bias voltage of +200 V (+400 V for ^{137}Cs) was supplied to the detector through the preamplifier, with the front surface of the crystal negatively biased in order to maximize the collection of holes. Output pulses were processed with a pulse-shaping amplifier having a $0.5\text{ }\mu\text{sec}$ shaping time and sent to a PC-based multi-channel analyzer.

2.3 Scoring of Electron-Hole Pair Collection

Electron-hole pairs are created whenever energy is deposited in a semiconductor. The average energy required to create an electron-hole pair is denoted as the W value (we used $W = 4.6\text{ eV}$ for the

CdZnTe). The output pulse is proportional to the charge that is collected which, in turn, is controlled primarily by the mobility-lifetime products, $\mu_e\tau_e$ and $\mu_h\tau_h$ (units: cm^2/V), for electrons and holes, respectively. The mobility of charge carriers in CdZnTe is much smaller than in Si and Ge detectors and, thus, the charge carriers are easily trapped in the crystal while they drift to the electrodes.

The charge-collection efficiency is defined as the ratio of the number of charge carriers collected at the electrodes to the total number of carriers generated by the radiation energy deposition. If the effect of detrapping is neglected, the charge-collection efficiency $\eta(z)$ for charge carriers at depth z in a semiconductor crystal of thickness d (cm) can be determined by means of the Hecht equation[4]:

$$\eta(z) = (\lambda_e/d)(1 - e^{-(d-z)/\lambda_e}) + (\lambda_h/d)(1 - e^{-z/\lambda_h}) \quad (1)$$

where $\lambda_e = \mu_e\tau_e E$ and $\lambda_h = \mu_h\tau_h E$ are the mean free paths (units: cm) for electrons and holes, respectively, z is the depth into the crystal from the negatively-biased (voltage V in volts) front surface and E is the electric field strength ($E=V/d$) in the detector.

Typical mobility-lifetime values we used in the Hecht equation were $\mu_e\tau_e = 7 \times 10^{-3} \text{ cm}^2/\text{V}$ and $\mu_h\tau_h = 5 \times 10^{-5} \text{ cm}^2/\text{V}$. With a high voltage of 200 V and a detector thickness of $d = 0.2 \text{ cm}$, the λ_e is 7 cm and λ_h is 0.05 cm. Therefore, it is clear that holes can be easily trapped particularly when they are produced at depths far away from the negatively-biased electrode.

Since the low-energy photons from ^{241}Am deposit energy primarily near the front face while the 662-keV photons of ^{137}Cs deposit energy uniformly along the depth, the charge collection effect is more pronounced for ^{137}Cs photons, which also makes it a better source to examine the effect of mobility-lifetime value.

2.4 Fano Factor and Electronic Noise Broadening

To compare the EGS4-calculated spectra with experimental results, the Fano factor and the peak broadening due to electronic noise, etc. were also considered[9]. Namely, for each incident photon, a running sum of the total number of electron-hole pairs that are created at the EDEP sites in the detector is kept with each contribution multiplied by the corresponding charge-collection efficiency determined by the Hecht equation. To be more specific, we first determine the charge collected (unstraggled) per photon event N :

$$N = \Sigma\eta(z)E_{dep}(z)/W, \quad (2)$$

where $E_{dep}(z)$ is the energy deposited at depth z from the front surface of the crystal. The total standard deviation is then determined from:

$$\sigma^2 = fN + \sigma_{enc}^2, \quad (3)$$

where f is the Fano factor for CZT and σ_{enc} is a standard deviation to account for the equivalent noise charge of the electronics[9]. We used values for W , f and σ_{enc} similar to those reported by Bencivelli et al.[10] for Cd-Te; $f=0.14$ and $\sigma_{enc}=150$ e-h pairs.

Finally, the straggled (broadened) charge that is collected, N_s , is statistically determined by sampling from a Gaussian peak, centered about N with σ . The corresponding energy, $E_s = WN_s$, is then histogrammed for each incident photon event for comparison with experiment.

3 Results

Figure 2 shows that ^{241}Am spectra calculated using EGS4 with the latest KEK low-energy photon production and transport routines and that with Nelson's approach for compounds (the previous study) have perfect agreement for the major peaks above 10 keV. Similar comparisons for ^{133}Ba and ^{109}Cd also gave good agreement. Hereafter throughout the paper the results will be those calculated using the EGS4 with the KEK routines.

Figure 3 indicates that, as expected, the choice of different values for parameters W , Fano factor f , and density ρ of CdZnTe did not affect the spectrum much.

The measured photon spectrum is shown in Figure 4 for ^{241}Am (+200 V and 0.5 μs) and Figure 5 for ^{137}Cs (+400 V and 0.5 μs).

To illustrate our response calculation algorithm, Figure 6 shows the ^{241}Am photon spectrum at different stages of CZT spectral response calculations. The top figure is the energy deposition spectrum, the middle one is the spectrum taking into account the charge collection and peak modification from Fano factor and electronic noise (but W value is not included yet), and the bottom one is the final photon spectrum with the W value included.

To examine the Hecht equation and its parameters, we first studied the effect of hole's mobility-lifetime value. Figure 7 shows three ^{241}Am photon spectra calculated using three values of $\mu_h\tau_h$ while Figure 8 gives three corresponding ^{137}Cs photon spectra. After comparing these calculated spectra with the measurements in Figure 4 and 5, it is clear that a $\mu_h\tau_h$ value of $5 \times 10^{-5} \text{ cm}^2/\text{V}$ gave better (not perfect yet) agreements for both cases of ^{241}Am and ^{137}Cs . The results using the other two extreme values (3×10^{-4} and 7×10^{-6}) are not correct. This seems to be consistent with the $\mu_h\tau_h$ values stated in [11,12].

Setting the $\mu_h\tau_h$ value at $5 \times 10^{-5} \text{ cm}^2/\text{V}$, Figure 9 shows the ^{241}Am photon spectra calculated with two different values of $\mu_e\tau_e$ (1×10^{-3} and $7 \times 10^{-3} \text{ cm}^2/\text{V}$) and σ_{enc} (150 and 200 e-h). A $\mu_e\tau_e$ value of 7×10^{-3} seems to be correct and the value of 1×10^{-3} gave a wrong peak position result. The choice of σ_{enc} at 150 and 200 e-h does not affect the results. Similar conclusions were obtained for the case of ^{137}Cs source.

4 Conclusions

In this study we have used EGS4 to simulate the response of a CZT crystal, mounted within a BNC connector, taking into account the incomplete collection of charge by means of the Hecht equation. We have found perfect agreement for the calculated spectra between the EGS4 with the latest KEK low-energy photon routines and the standard EGS4 with Nelson's approach for compounds. This study has also shown that all of the photo and escape peaks appear at the correct energies, but the peak widths are not in perfect agreement with experiment. The most important parameter, mobility-lifetime for hole $\mu_h\tau_h$, should be around $5 \times 10^{-5} \text{ cm}^2/\text{V}$, while the mobility-lifetime for electron $\mu_e\tau_e$, should be about $7 \times 10^{-3} \text{ cm}^2/\text{V}$. The other parameters do not affect the spectra as much as the mobility-lifetime value. The remaining discrepancy may be due to that the Hecht model itself is too simple.

References

- [1] W. R. Nelson, T. Borak, R. Malchow, W. Toki and J. Kadyk, “EGS4 calculations for a CdZnTe detector to measure synchrotron radiation at PEP-II”, Proceedings of the First International Workshop on EGS4, KEK, Tsukuba, Japan, August 26-29, 1997.
- [2] W. R. Nelson, H. Hirayama and D. W. O. Rogers, “The EGS4 Code System”, *SLAC Report 265*, 1985.
- [3] A. Del Guerra, W. R. Nelson and P. Russo, “A simple method to introduce K-Edge sampling for compounds in the code EGS4 for x-ray element analysis”, *Nucl. Instr. Meth.* **A306**(1991)378, [Erratum: *Nucl. Instr. Meth.* **A359**(1995)637].
- [4] G. Baldazzi, D. Bollini, F. Casali, P. Chirco, A. Donati, W. Dusi, G. Landini, M. Rossi and J. B. Stephen, “Timing response of CdTe detectors”, *Nucl. Instr. Meth.* **A326**(1993)319.
- [5] H. Hirayama and Y. Namito, “Implementation of a general treatment of photoelectric-related phenomena for compounds or mixtures in EGS4”, KEK Internal 2000-3, 2000.
- [6] Y. Namito and H. Hirayama, “LSCAT: low-energy photon-scattering expansion for the EGS4 code (inclusion of electron impact ionization)”, KEK Internal 2000-4, 2000.
- [7] A. F. Bielajew and D. W. O. Rogers, “PRESTA: The Parameter Reduced Electron Step Transport Algorithm for Electron Monte Carlo Transport”, *Nucl. Instr. Meth.* **B18**(1987)165; also *NRC-PIRS-0042*, 1986.
- [8] Radioactive Transformations, Publication 38, International Commission of Radiological Protection, *Annals of the ICRP 11-13*, 1983.
- [9] W. R. Leo, *Techniques for Nuclear and Particle Physics Experiments* (Springer-Verlag, Second Edition, 1994; see Chapter 10.
- [10] W. Bencivelli, E. Bertolucci, U. Bottigli, A. Del Guerra, A. Messineo, W. R. Nelson, P. Randaccio, V. Rosso, P. Russo and A. Stefanini, “Evaluation of elemental and compound semiconductors for x-ray digital radiography”, *Nucl. Instr. Meth.* **A310**(1991)210.
- [11] H. Nishizawa, et al., “Calculation of CdTe semiconductor detector response”, Proceedings of the First International Workshop on EGS4, KEK, Tsukuba, Japan, August 26-29, 1997.
- [12] G. A. Johansen and E. Abro, “A new CdZnTe detector system for low-energy gamma-ray measurement”, *Sensors and Actuators* **A54**(1996)493-498.

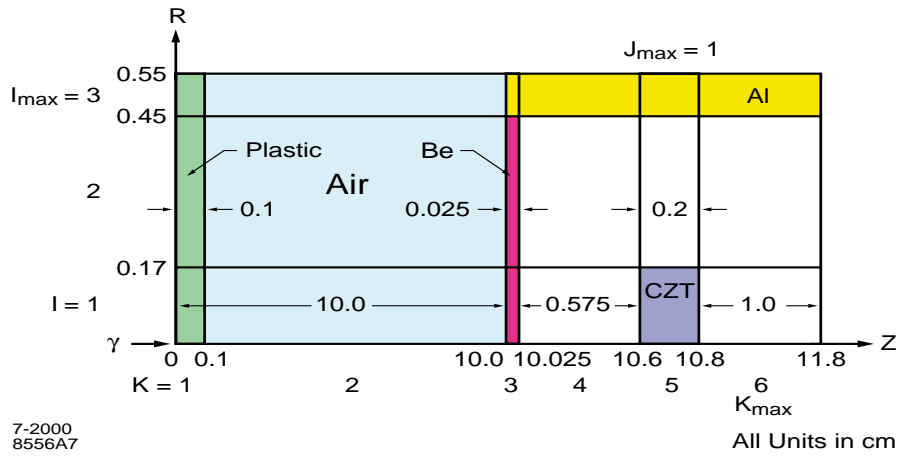


Figure 1. Irradiation geometry for the CdZnTe detector using ^{241}Am and ^{137}Cs disk sources.

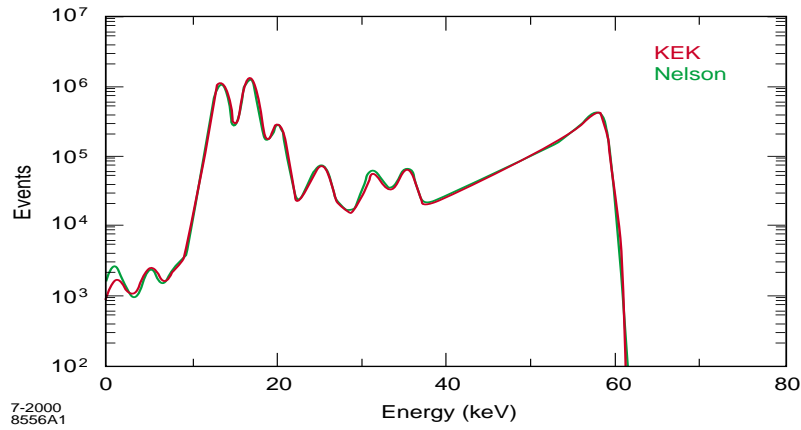


Figure 2. Comparison of ^{241}Am spectra calculated with EGS4 using two different schemes; the latest KEK low-energy photon production and transport routines and Nelson's approach for compounds.

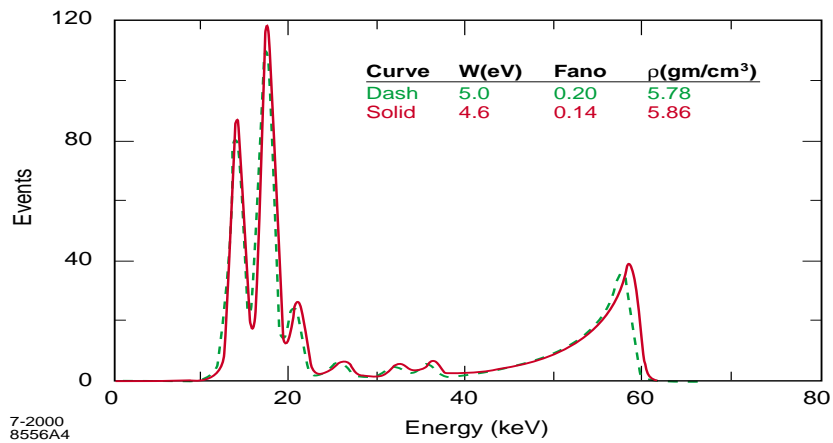


Figure 3. Comparison of ^{241}Am spectra calculated with EGS4 (with the KEK low-energy photon routines) using different values for parameters of W , Fano factor f , and density ρ of CdZnTe.

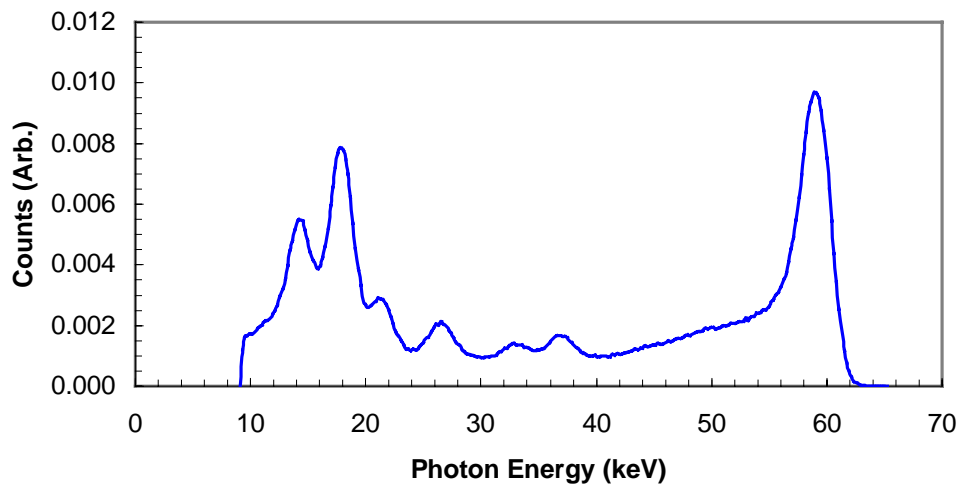


Figure 4. ^{241}Am photon spectrum measured using CdZnTe detector (+200 V and 0.5 μs).

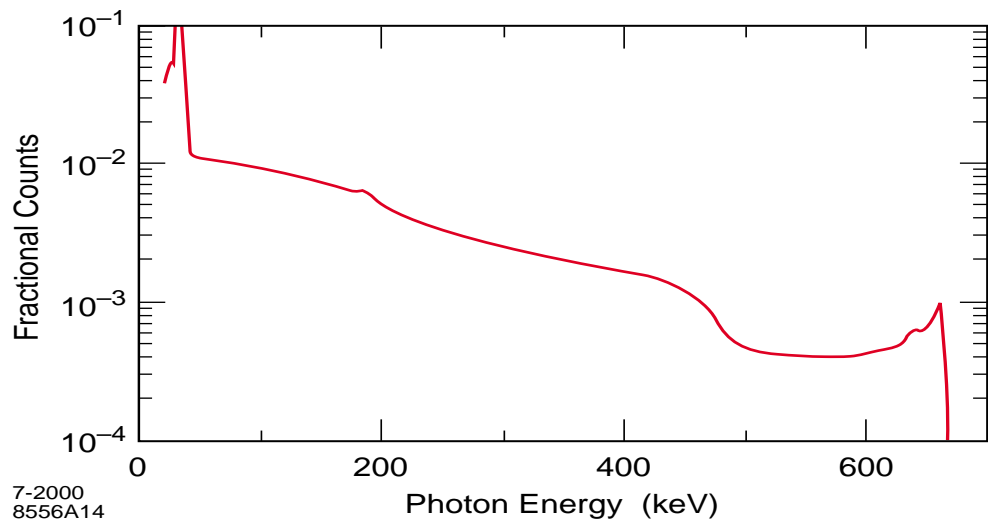


Figure 5. ^{137}Cs photon spectrum measured using CdZnTe detector (+400 V and 0.5 μs).

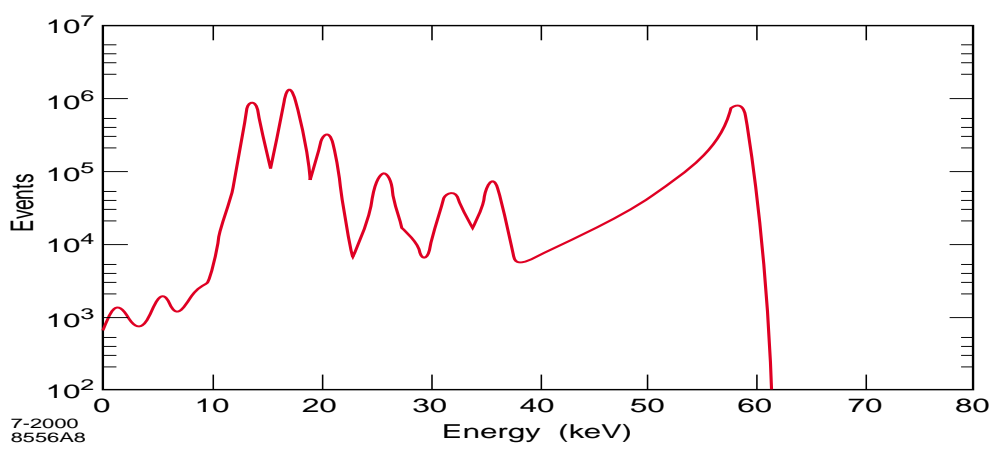
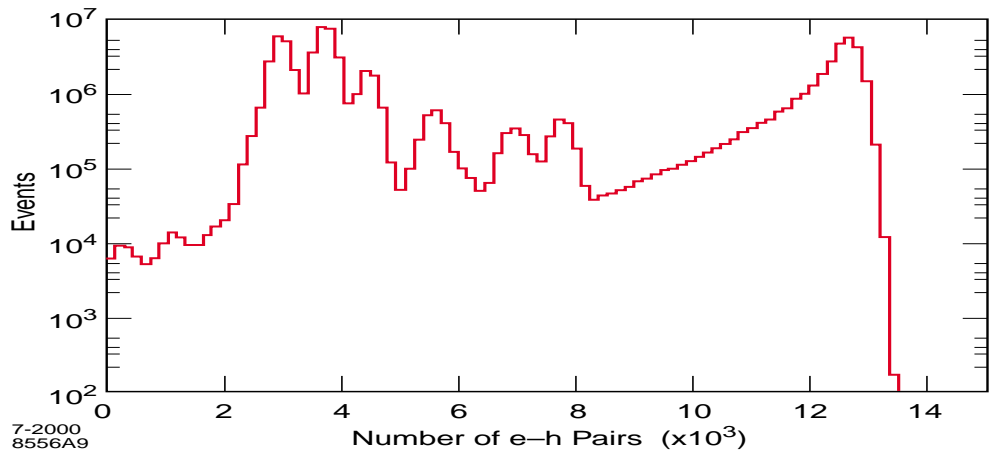
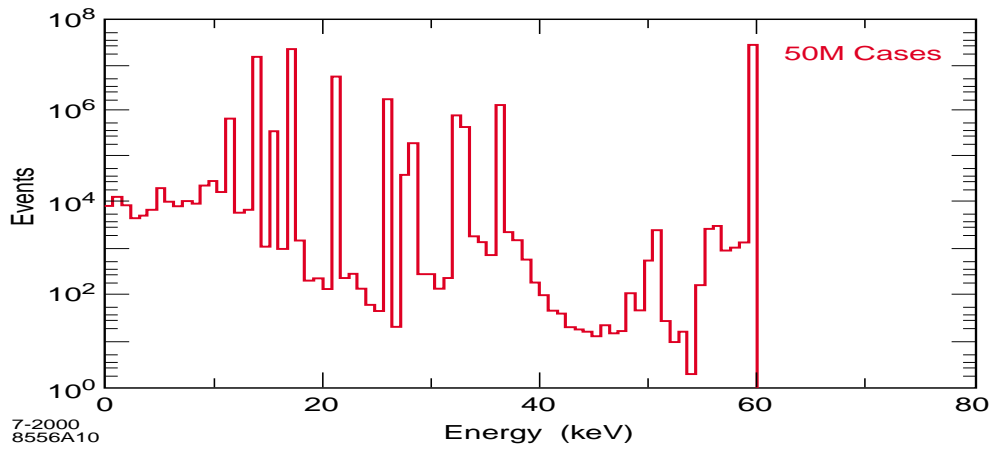


Figure 6. ^{241}Am photon spectrum at three stages of CdZnTe response calculation: energy deposition spectrum (top), electron-hole pair spectrum (middle), and photon spectrum (bottom).

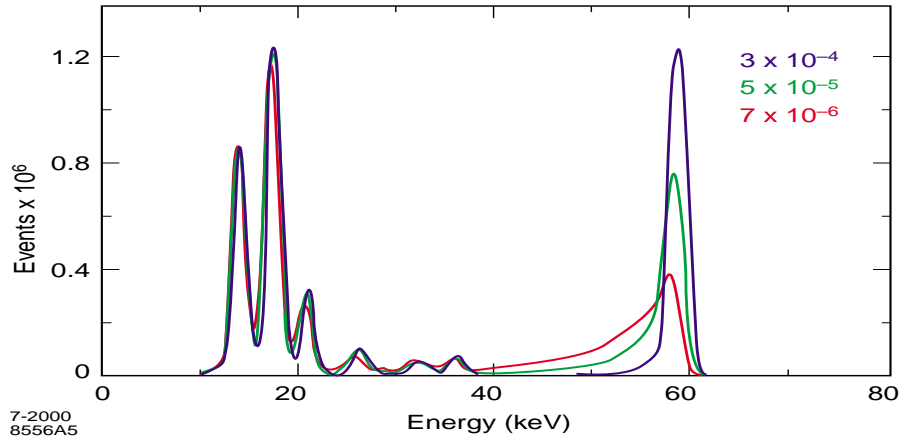


Figure 7. ^{241}Am photon spectrum calculated with EGS4 using three values of $\mu_h\tau_h$ (units in cm^2/V).

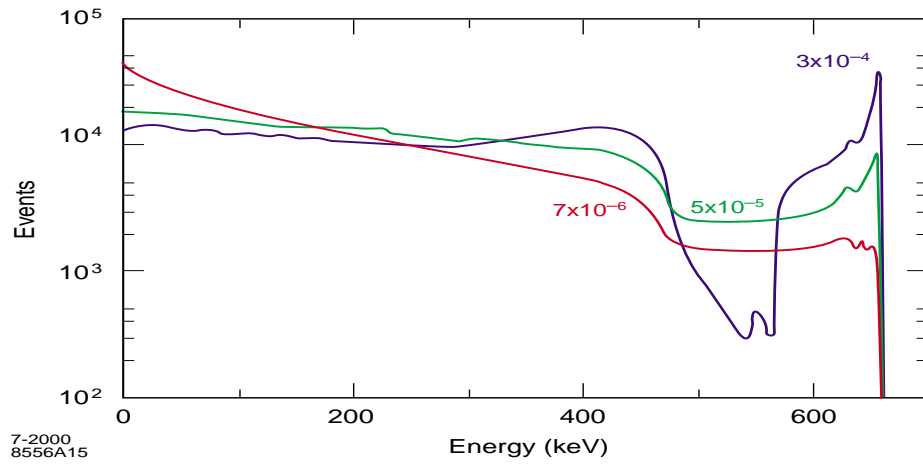


Figure 8. ^{137}Cs photon spectrum calculated with EGS4 using three values of $\mu_h\tau_h$ (units in cm^2/V).

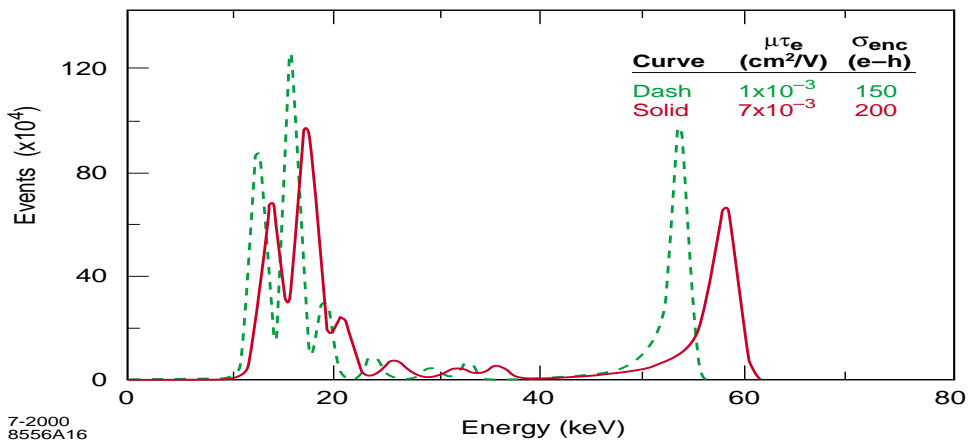


Figure 9. ^{241}Am photon spectrum calculated with EGS4 using different values of $\mu_e\tau_e$ and σ_{enc} .